fibers

MDPI

Article

High-Pressure Hydrogen Influence on Cellulose Nanofibers Filled Nitrile Rubber: Performance in Storage Applications

Sheng Ye [1], Sohail Yasin [1,2,*], Haijie Zhi [1], Yihu Song [3], Chaohua Gu [1] and Jianfeng Shi [1,2,*]

[1] Institute of Process Equipment, Zhejiang University, Hangzhou 310027, China; zjusheng@zju.edu.cn (S.Y.); 22427029@zju.edu.cn (H.Z.); guchaohua@zju.edu.cn (C.G.)
[2] Hydrogen Energy Research Institute, Zhejiang University, Hangzhou 310027, China
[3] Department of Polymer Science and Engineering, Zhejiang University, Hangzhou 310027, China; s_yh0411@zju.edu.cn
* Correspondence: soh.yasin@gmail.com (S.Y.); shijianfeng@zju.edu.cn (J.S.)

Abstract: High-pressure hydrogen storage systems (up to 100 MPa) require advanced materials for safety and reliability, particularly for rubber seals, which are prone to degradation under extreme conditions. This study explores the use of cellulose nanofibers (CNFs) and cellulose nanocrystals (CNCs) as sustainable nanofillers for nitrile butadiene rubber (NBR) latex nanocomposites. CNFs and CNCs were evaluated for their effects on mechanical properties, crosslink density, and resistance to high-pressure hydrogen exposure in rubber O-rings. A life cycle assessment (LCA) was carried to assess the environmental impact of these nanocomposites. The results showed that CNF-filled NBR composites exhibited better resistance to bubble formation under hydrogen exposure compared to CNC-filled ones. However, the LCA indicated relatively high environmental impacts for both, reaching up to 2.5 kg CO_2 eq. in Global Warming Potential (GWP), highlighting the need for further optimization of production processes. This study demonstrates the potential of cellulose nanofillers to improve NBR performance while advancing sustainable hydrogen storage materials.

Keywords: cellulose nanofibers; rubber O-rings; mechanical properties; high pressure; hydrogen exposure

check for updates

Academic Editor: Shingo Yokota

Received: 31 December 2024
Revised: 21 February 2025
Accepted: 3 March 2025
Published: 5 March 2025

Citation: Ye, S.; Yasin, S.; Zhi, H.; Song, Y.; Gu, C.; Shi, J. High-Pressure Hydrogen Influence on Cellulose Nanofibers Filled Nitrile Rubber: Performance in Storage Applications. *Fibers* **2025**, *13*, 29. https://doi.org/10.3390/fib13030029

Copyright: © 2025 by the authors. Licensee MDPI, Basel, Switzerland. This article is an open access article distributed under the terms and conditions of the Creative Commons Attribution (CC BY) license (https://creativecommons.org/licenses/by/4.0/).

1. Introduction

The hydrogen energy sector is advancing toward industrial-scale deployment; however, significant challenges remain due to hydrogen's high volatility and low density. High-pressure hydrogen storage systems require advanced materials to ensure safety and reliability. Rubber seals, which are critical components in these systems, are particularly vulnerable to degradation under pressures up to 100 MPa [1]. This degradation often manifests as swelling, blistering, and cracking, causing structural failure. Nitrile butadiene rubber (NBR) is commonly used in such seals due to its excellent resistance to oils, fuels, and nonpolar gasses, as well as its low gas permeability. In addition to rubber, nanofillers play a vital role in enhancing the stability and functionality of materials used in high-pressure hydrogen storage. Conventional nanofillers like carbon black (CB) and silica contribute to mechanical reinforcement but are known to absorb hydrogen, which can negatively affect material performance [2,3]. Furthermore, these nanofillers have significant environmental impacts, posing sustainability challenges [4]. A promising solution lies in the use of sustainable nanofillers, such as cellulose-based nanomaterials [5].

Cellulosic polymer nanocomposites are materials where cellulose-derived nanofillers are added into polymers to improve their thermal and mechanical properties. Due to their abundance and renewability, cellulosic nanofibrillar structures have attracted significant attention over the past two decades. Cellulose nanofillers are primarily sourced from wood, agricultural residues, and bacterial cellulose. They are notable for their biodegradability, high strength, and Young's modulus, making them widely used in nanocomposite development. Numerous studies have focused on preparing and characterizing elastomer-based nanocomposites reinforced with nanocellulose [6]. Various rubbers, including natural rubber (NR), epoxidized natural rubber (ENR), styrene-butadiene rubber (SBR), and butadiene rubber (BR), have been enhanced for mechanical, thermal, gas barrier, and dynamic mechanical properties [7]. Acrylonitrile butadiene rubber (NBR) is a polar rubber known for its heat resistance, high compression set, oil resistance, and abrasion resistance. It is commonly used in products like seals, hoses, and gloves, though it is not biodegradable and lacks strain-induced crystallization [7].

This study investigates the development of NBR latex nanocomposites incorporating cellulose nanofillers for high-pressure hydrogen sealing applications, with a focus on rubber O-rings. Cellulose nanofibers (CNFs) and cellulose nanocrystals (CNCs) are explored as sustainable alternatives to traditional nanofillers. The research uses NBR latex formulations by varying the type of cellulose nanofillers to evaluate their effects on mechanical properties, crosslink density (v_c), and performance under high-pressure hydrogen exposure. Additionally, the low-carbon manufacturing potential of these nanocomposites is assessed through a life cycle assessment (LCA), demonstrating the potential of cellulose nanofillers to enhance the performance of NBR nanocomposites while reducing environmental impact, thereby enabling sustainable and low-carbon manufacturing solutions for hydrogen storage systems.

2. Materials and Methods

Nitrile butadiene rubber latex (NBR) is derived from butadiene, acrylonitrile, unsaturated carboxylic acids, and other additives through emulsion polymerization with a solid content of 43–45% and a density of 0.91 g/cm^3. It was sourced from Dongguan Jiaqing Plastic Raw Materials Co., Ltd., Dongguan, China. For the reinforcing filler, CNC, with lengths from 140 to 200 nm and diameters between 5 and 20 nm, and CNF, with a 50 nm diameter and lengths up to several hundred microns, were acquired from Cellulose Lab., Canada. They were supplied in aqueous suspensions of 12.0% (CNC) and 3.0% (CNF). N-(1,3-dimethylbutyl)-N-phenyl-p-phenylenediamine (6PPD), used as antioxidant, was sourced from Anzhe Chem. Co. Ltd., Suzhou, China. The vulcanizing agents and additives, including sulfur and zinc oxide (ZnO), were attained from Zhejiang Yongjia Chem. Co. Ltd., Wenzhou, China, and Aladdin Ind. Co., Shanghai, China.

2.1. Cellulose-Filled NBR Sample Preparations

NBR nanocomposites from the latex were prepared following the formulation outlined in Table 1, where the cellulose nanofiller suspension was mixed directly into the latex. The suspension was gradually added drop by drop into a beaker containing NBR latex, with continuous stirring for 2 h. The latex containing cellulose nanofillers was oven-dried for 12 days at 40 °C. The nanocomposites were prepared using the dried NBR latex rubber in an internal mixer (HOOK, Shanghai Kechuang Co. Ltd., Shanghai, China). Initially, antioxidant 6PPD was blended at 100 °C for 20 min at an extruder speed of 40 rpm. Afterward, sulfur and zinc oxide were introduced and mixed at 100 °C for another 10 min to complete the formulation. Sheets of vulcanized NBR for characterization were produced by compressing the compound mixture at 12 MPa using a vulcanizer (XL-25, Huzhou Xinli

Rubber Machinery Co. Ltd., Huzhou, China). The sheets were compressed to a thickness of around 2.0 mm at 150 ± 5 °C for 30 min.

Table 1. Formulation used for Neat NBR and CNC or CNF filled nanocomposites from the latex.

Process	Time	NBR	PPD	Sulfur	Zn	CNC	CNF
Latex mixing (27 °C)	0 s	400 g	0	0	0	0 or 50 mL *	0 or 200 mL *
Drying (40 °C)	The latex was dried for 12 days						
Internal mixing (100 °C)	2400 s	190 g	2 g	4 g	2 g	0	0
Milling (27 °C)	The prepared compound was milled for 600 s						
Sheeting (150 °C)	The compound was compressed at 15 MPa for 600 s						

* Neat NBR: CNC = 0 mL, CNF = 0 mL; CNC filled NBR: CNC = 50 mL, CNF = 0 mL; CNF filled NBR: CNC = 0 mL, CNF = 200 mL.

2.2. Hydrogen Exposure and Characterization

The prepared rubber nanocomposites were subjected to hydrogen exposure at 100 MPa for 4 h. The samples were exposed to 99.99% hydrogen in a hydraulic servo-controlled testing machine equipped with an autoclave [1,4]. The samples before and after hydrogen was exposed were characterized for their morphological and mechanical properties, including crosslinking density (v_c). v_c was measured according to Flory–Rehner equation $v_c = -\frac{ln(1-v_r)+v_r+\chi_1 v_r^2}{V\left(v_r^{1/3}-v_r/2\right)}$ [8,9]. Here, V = 106.4 cm^3/mol represents the molar volume of toluene, and χ_1 is the Flory–Huggins parameter of interaction, which is taken as 0.6 for NBR. The volume fraction of the rubber, *vr*, is calculated based on the following method: $v_r = \frac{\rho_s\left(m_2-w_f m_0\right)}{\rho_s\left(m_2-w_f m_0\right)+\rho_r(m_1-m_2)}$. The weight fraction of nanofillers in the NBR nanocomposite is denoted as wf, and the weights of the samples in their initial (m_0), swollen (m_1), and de-swollen (m_2) states were measured. The densities of toluene (ρs = 0.887 g/mL) and NBR (ρr = 0.970 g/mL) were used for the calculations. As a mechanical characterization of all elastic properties is essential for enhancing design optimization [10], uniaxial tensile tests were performed on NBR nanocomposites at room temperature using dog-bone-shaped specimens with dimensions of 35 mm in length, 2 mm in width, and 2 mm in thickness. The tests were conducted on an electronic universal testing machine (SANS Tech, Shenzhen, China) with a crosshead speed of 50 ± 5 mm/min, following the guidelines of ASTM D 412 standards. Fourier-transform infrared (FTIR) spectroscopy of the NBR nanocomposites and samples exposed to hydrogen at 50 MPa was performed with a spectrometer (Nicolet iS10, Thermo Fisher Scientific Inc., Waltham, MA, USA). The scans were performed with 32 co-additions, covering a range of 4000 cm^{-1} to 500 cm^{-1}, and a resolution of 2 cm^{-1} was used.

2.3. LCA of Cellulose-Filled NBR Manufacturing

Life cycle assessment (LCA) was carried to evaluate the environmental impacts of NBR nanocomposites used for O-rings during the manufacturing phase, including raw material acquisition and processing. This study primarily focused on the manufacturing phase of rubber nanocomposites, starting from raw material acquisition to the production of the final products, using a defined functional unit (FU) of 1 kg. The goal was to measure the environmental impact of the manufacturing phase for rubber nanocomposites, specifically those made with cellulose-based NBR, aiming to highlight contributions toward low-carbon manufacturing, energy conservation and future improvements for high-performance rubber nanocomposites in high-pressure hydrogen applications. For this study, a 1 kg FU of rubber made from NBR nanocomposites including raw materials (NBR, sulfur, zinc, and cellulose acetate fibers) and energy inputs and outputs was referenced in the "gate-to-gate" LCA.

2.3.1. Lifecycle Inventory (LCI) Analysis

The LCI phase involved collecting data to track material [11] and energy flows across the manufacturing stages of NBR nanocomposites, with compression molding and hot internal mixing to produce vulcanized rubber nanocomposites. The experimental results provided primary data, were allocated based on product mass prepared in the lab. Data on material flows (NBR, cellulose acetate fibers, sulfur, and zinc) and energy usage (electricity mix, China) were sourced using demo EIME software v6.0 [12], supplemented with updated EN 15804+A2 and CODDE databases.

2.3.2. Lifecycle Impact Assessment (LCIA)

The LCIA phase integrated LCI data and elementary flows to evaluate environmental impacts by categorizing and characterizing the results across 17 midpoint impact categories [4]. The impact categories that were normalized include the following: total climate change (GWP), biogenic climate change (GWPb), fossil climate change (GWPf), acidification (AP), ozone depletion (ODP), marine eutrophication (Epm), freshwater eutrophication (Epf), terrestrial eutrophication (Ept), resource use of minerals and metals (ADPe), photochemical ozone formation, human health (POCP), fossil resource use (ADPf), water use (WU), ionizing radiation for human health (IR), particulate matter (PM), human toxicity related to cancer (CTUh-c), ecotoxicity in freshwater (CTUe), and human toxicity related to non-cancer (CTUh-nc). The midpoint approach enabled comparative evaluations of production processes across all impact categories [13], facilitating a deeper understanding of environmental trade-offs and improvement opportunities in rubber nanocomposites for O-ring manufacturing.

3. Results

Figure 1a–f illustrates the morphology of NBR nanocomposites before and after exposure to 100 MPa high-pressure hydrogen for 4 h. NBR exhibited the formation of bubbles, which increased in the CNC-filled NBR, while the CNF-filled NBR retained its microstructure under the same conditions. The bubbles are attributed to internal fractures caused by rapid decompression of high-pressure hydrogen [2]. The CNF-filled nanocomposites showed no bubble formation but swelled to twice the size of the NBR and CNC-filled nanocomposites, suggesting enhanced hydrogen escape during decompression.

Hydrogen-induced blister fracture after hydrogen exposure is a critical failure mode for rubber O-rings in high-pressure hydrogen systems. During hydrogen exposure, hydrogen molecules dissolve into the rubber matrix and accumulate at microstructural flaws such as cavities and filler interfaces [14–16]. When the external pressure decreases, the dissolved hydrogen becomes supersaturated, resulting in rubber swelling and the formation and growth of bubbles. These bubbles cause local stress concentration. Once the stress exceeds the cohesive strength of the rubber, microcracks initiate and propagate, forming blisters on the surface or within the material. Fillers can affect the hydrogen mechanical properties and transport properties of rubber, ultimately influencing its resistance to hydrogen-induced blister fracture. The effects of CB and silica nanofillers on the blister fracture of EPDM and NBR exposed to 10 MPa hydrogen are known to alter the blister fracture depending on the content and type of nanofiller used [16]. In fact, fillers enhanced the tensile properties of the rubber. However, cellulose nanofillers have strong hydrophilicity, which causes them to easily agglomerate in the rubber matrix [17]. These agglomeration sites may serve as locations for hydrogen gas accumulation, leading to hydrogen-induced blistering. This could be the reason why the blistering in CNC-filled NBR is more severe than in neat NBR.

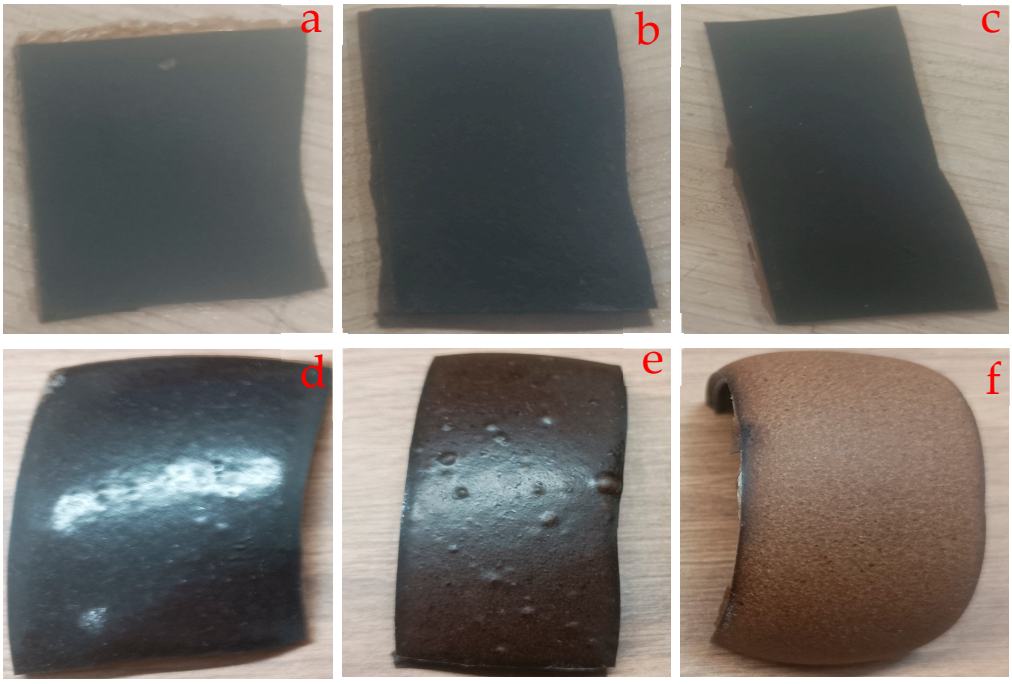


Figure 1. Images of NBR (**a**,**d**) and CNC (**b**,**e**) or CNF (**c**,**f**) filled nanocomposites before (**a**–**c**) and after (**d**–**f**) 99.99% high-pressure hydrogen exposure at 100 MPa for 4 h.

From the images in Figure 1, it is evident that the morphology of the NBR and the fillers in the NBR matrix are significantly influenced by hydrogen exposure. The numerous pores appeared in neat NBR, and the matrix appears relatively clean due to the lack of filler. The number of pores and bubbles in the CNC-filled NBR increases, likely due to trapped hydrogen at the interface of filler or curative agglomerates within the NBR matrix [1,2]. The overall sample bulging or swelling observed in CNF-filled NBR, rather than pores and bubbles, may be attributed to the higher surface area of CNF compared to CNC. This is because CNFs are more fibrous and have a larger surface area due to their longer, more flexible structure, whereas CNCs have a relatively compact and crystalline structure. The shape factor and filler volume fraction of the fillers are known to influence cavity nucleation or bubble formation in rubber materials when exposed to high gas pressure [18,19].

Studies have classified the interactions between nanocellulose fillers and NBR chains into two main types: (1) hydrogen bonding interactions, where the abundant OH groups on the surface of CNs allow for the attachment of NBR chains, particularly through interactions between the OH groups and the C≡N groups of the NBR; and (2) physical adsorption, which is enhanced by the nanoscale of the CNs and the similar polarity between CNs and NBR chains. This interaction reduces the mobility of the polymer chains and functions as a multifunctional cross-linker [20,21]. Similarly, the interactions between the nanofillers (CNC or CNF) and the rubber matrix were investigated using FTIR spectroscopy, as illustrated in Figure 2. The FTIR spectra of neat NBR show transmission peaks at 2920–2841 cm^{-1}, later slightly shifted to 2922–2845 cm^{-1} with the addition of nanofillers, which are attributed to asymmetric and symmetric –CH vibrations. The peak at 964 cm^{-1} is associated with C-H stretching of the butadiene double bond (–CH=CH (trans)). Additional peaks at 1440 and 1098 cm^{-1} are attributed to $–CH_2$ bending and C-O stretching vibrations, respectively. The utilization of the glycosidic rings of nanofiller chains at 1080 cm^{-1} and the transition of the peak from 2232 cm^{-1} to 2236 and 2238 cm^{-1} indicate effective interaction between the –CN functional groups of NBR and the –OH functional groups of CNC or CNF-filled nanocomposites [7,22]. After hydrogen exposure at 100 MPa, the neat NBR and nanofiller-filled nanocomposites were found to be benign

without any significant changes. However, slight changes in intensity and position were observed in the peaks—1098 cm^{-1}, 1080 cm^{-1}, 2002 cm^{-1}, 2232 cm^{-1}, 2236 cm^{-1}, and 2238 cm^{-1}—indicating further structural modifications after hydrogen exposure.

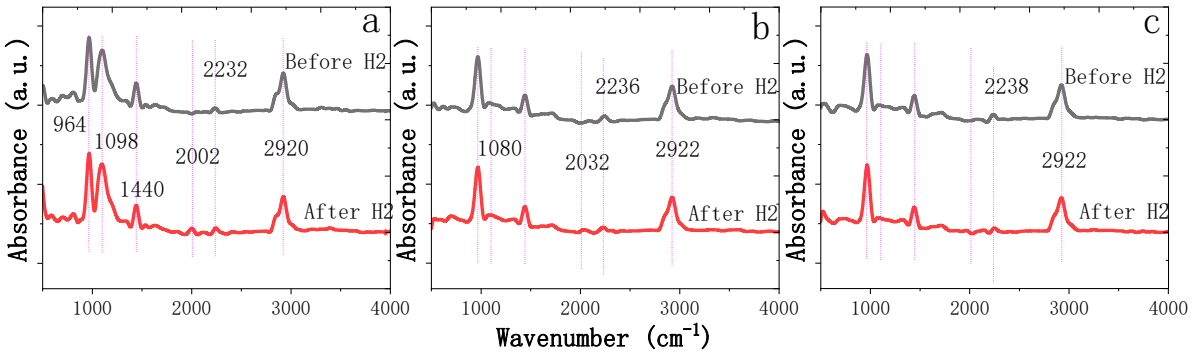


Figure 2. FTIR spectra of NBR (**a**) CNC (**b**) or CNF (**c**) filled nanocomposites before and after 99.99% high-pressure hydrogen exposure at 100 MPa for 4 h.

Figure 3 illustrates the σ-ε curves of NBR and CNC or CNF-filled nanocomposites. The addition of CNC increased the ε, while CNF synergistically increased σ and ε. The reinforcement of CNF on the reinforcement is evident, leading to an increase in tensile strength. However, after hydrogen exposure, not much change was seen in neat NBR, yielding a cumulative σ-ε curve recovery and earlier ε. The CNF-filled nanocomposites showed more recovery compared with CNC-filled NBR nanocomposites. Hydrogen acts as a reducing gas and facilitates hydrogenation reactions. Under high-pressure conditions, unexpected reactions can occur because the energy supplied by pressurization exceeds the activation energy required to transition rubber molecules into an activated state. Changes in the mechanical properties of CNC and CNF-filled NBR may suggest varied hydrogenation in the samples, as hydrogen significantly influences NBR, leading to up to 70% of NBR being converted into hydrogenated HNBR upon high-pressure hydrogen exposure [15,23]. Moreover, hydrogenated HNBR exhibits an ultimate strength 12 times greater than that of NBR, along with an increase in its glass transition temperature during the hydrogenation process [24].

Nanofillers significantly influence the mechanical properties of nanocomposites; thus, the v_c and SR were evaluated both before and after exposure to high-pressure hydrogen. Figure 4 illustrates the v_c and SR for the neat NBR and CNC or CNF-filled NBR, providing insights into the affinity of the cellulose nanofillers for the rubber chains. Strong interfacial interactions between the cellulose nanofillers and the rubber result in enhanced resistance to toluene absorption [25,26], increasing the v_c and lowering the SR. The notable enhancement in the v_c for NBR-CNF suggests that a higher aspect ratio filler of CNF facilitates greater v_c, resulting in a lower volumetric swelling ratio (Figure 4c,d) for NBR-CNC. Consequently, the swelling-induced elongation of the rubber molecular chains is reduced, and the ability of the solvent to infiltrate the free volume within the rubber matrix is reduced, also reducing SR. CNFs have a higher aspect ratio than CNCs due to their long, flexible, and entangled structure, which includes both crystalline and amorphous regions. This difference makes CNFs better for reinforcement in composites, as their high aspect ratio and larger surface area improve v_c and stress transfer and mechanical properties.

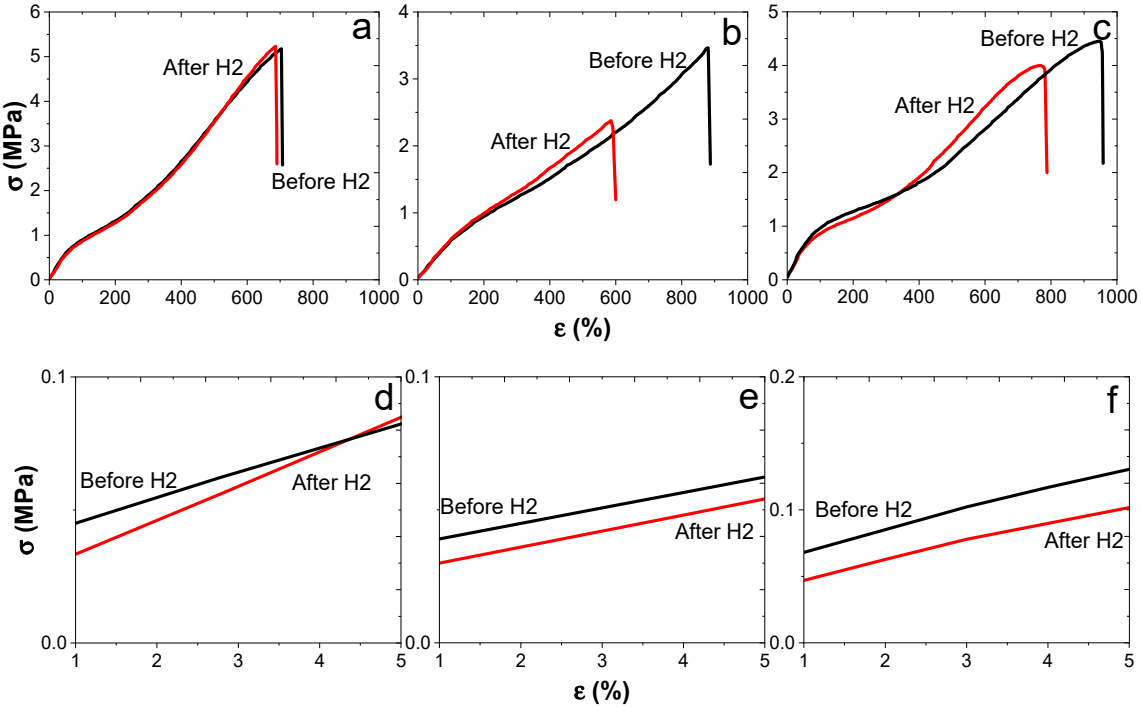


Figure 3. σ-ε curves (**a**–**c**) and σ at earlier ε (**d**–**f**) of NBR (**a**,**d**) and CNC (**b**,**e**) or CNF (**c**,**f**) filled nanocomposites before and after 99.99% high-pressure hydrogen exposure at 100 MPa for 4 h.

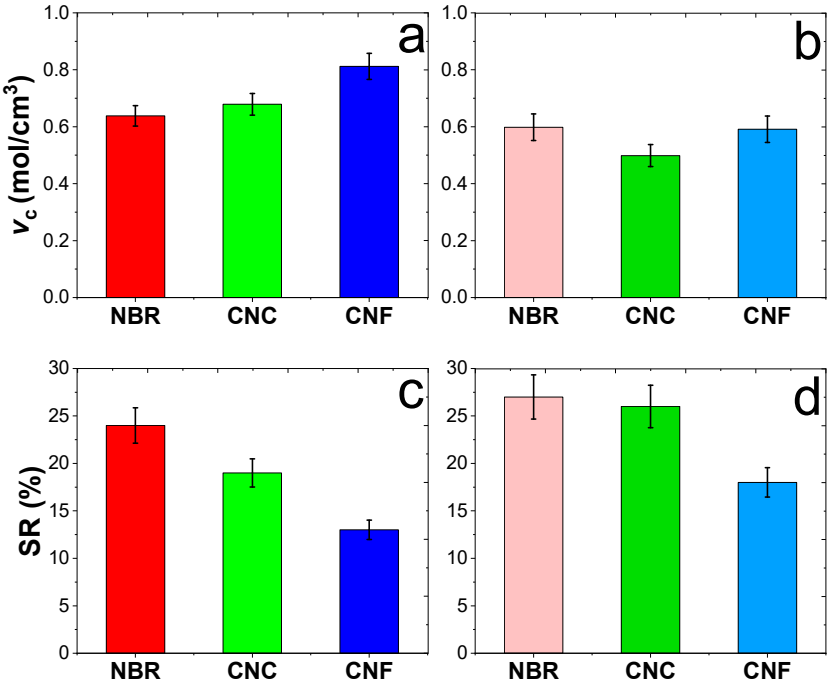


Figure 4. Crosslinking density (v_c) (**a**,**b**) and sol ratio (**c**,**d**) of NBR and CNC or CNF-filled nanocomposites before (**a**,**c**) and after (**b**,**d**) 99.99% high-pressure hydrogen exposure at 100 MPa for 4 h.

The normalized σ-ε plots, which represent σ/(vcRT) versus ε, are presented in Figure 5, where T is the absolute temperature and R is the gas constant. The dependency of neat NBR nanocomposites on v_c is visible, even after high-pressure hydrogen exposure, which is associated with the retained networks. Following the high-pressure hydrogen exposure at 100 MPa for 4 h, network defects reduce the v_c of NBR nanocomposites containing CNC

or CNF. The dependency on v_c of samples prior to hydrogen exposure, which diminishes after exposure, is likely due to a reduction in crosslinked networks.

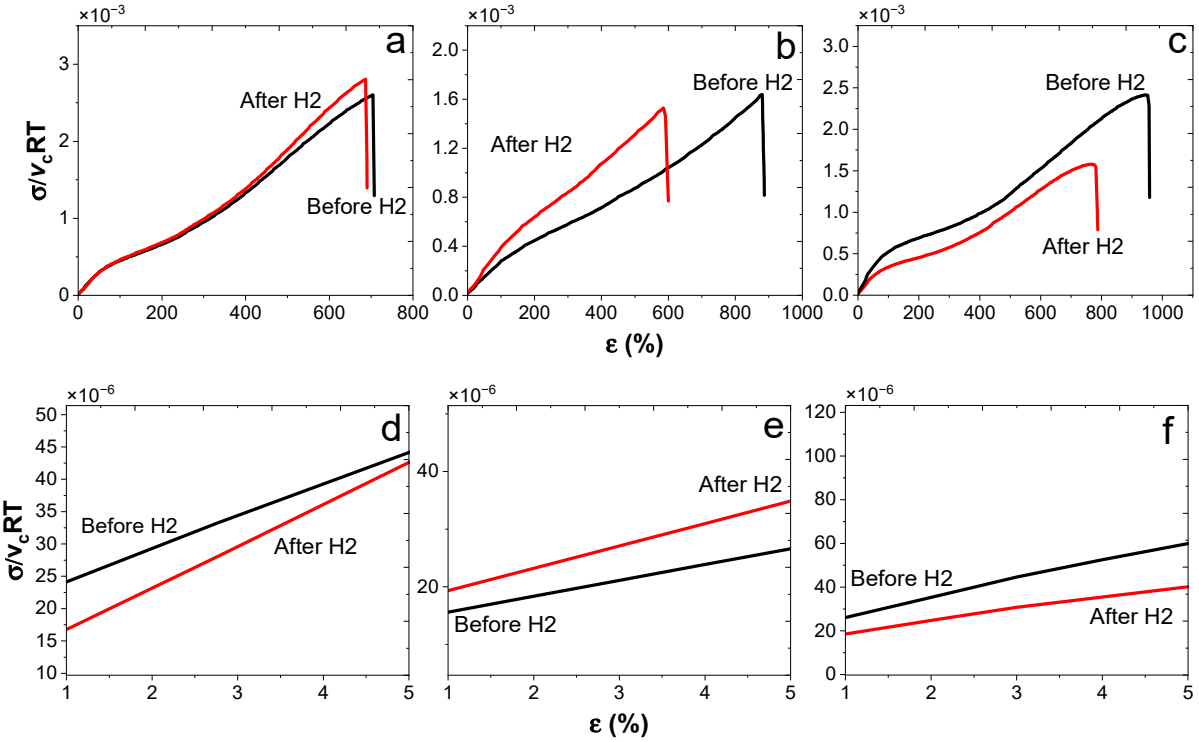


Figure 5. Normalized $\sigma/(v_cRT)$ against ε of tensile curves (**a**–**c**) and at earlier (**d**–**f**) of NBR (**a**,**d**) and CNC (**b**,**e**) or CNF (**c**,**f**) filled nanocomposites before and after 99.99% high-pressure hydrogen exposure at 100 MPa for 4 h.

The environmental impacts associated with the manufacturing phase of NBR-based nanocomposites filled with cellulose fibers are evaluated across 17 midpoint categories, as shown in Figure 6. The comparatively low toxicological profile of CNC and CNF relative to carbon black or silica suggests a reduced potential for environmental and health hazards. The electricity consumption for manufacturing one kilogram of NBR product (gloves) can reach up to ~10 MJ [27]. Moreover, the energy-intensive processes required for the production of cellulose fibers (micro- and nano-scale) substantially contribute to the overall environmental impact, highlighting the significant energy demand associated with their synthesis and processing [28,29]. Consequently, for the production of 1 kg of CO_2-based rubber, emissions range from 4.57 kg CO_2 eq, in the best-case allocation scenario, and 4.83 kg CO_2 eq in the worst-case allocation scenario [30]. The earlier LCA studies on CNF focused on a cradle-to-gate assessment for producing one ton of CNF, utilizing sulfite pulp as the raw material and comparing various distinct processing routes. These studies highlight significant differences in wastewater production across the different processing routes for the production of CNF. The enzymatic pre-treatment process produced higher yields but required more energy compared to other chemical pre-treatment methods [31]. Addition of cellulose fibers to the NBR nanocomposites, increases Global Warming Potential (GWP) from 2.3 to 2.5 kg CO_2 eq., primarily due to increased reliance on resources during processing. Adding bio-based cellulose nanofillers in NBR nanocomposite manufacturing increases several environmental impacts, notably in Ept (eutrophication of freshwater, marine, and terrestrial environments.

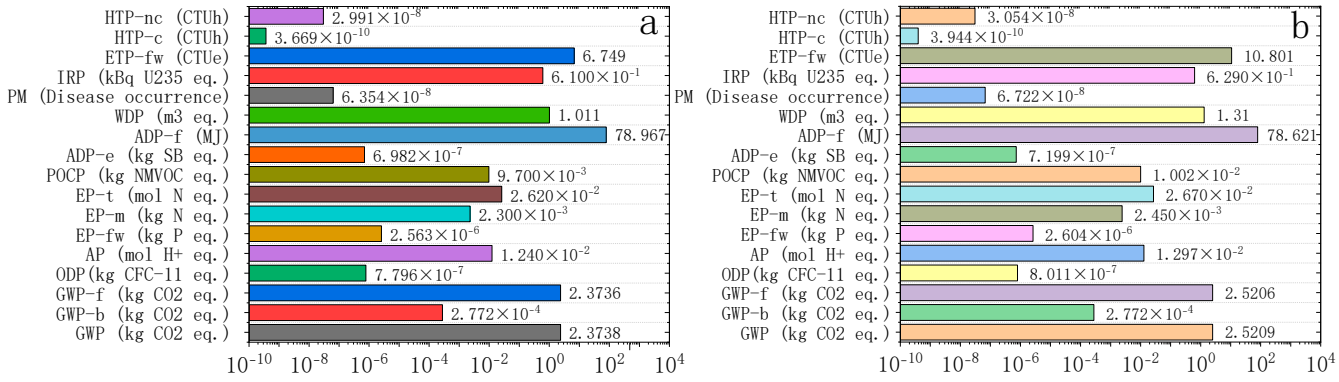


Figure 6. Gate-to-gate midpoint assessment of NBR (**a**) and cellulose fibers filled nanocomposites manufacturing phase (**b**).

4. Conclusions

This study highlights the promising potential of CNFs and CNCs as sustainable nanofillers for enhancing the performance of NBR latex composites in high-pressure hydrogen storage systems, particularly for rubber O-rings. The incorporation of CNFs significantly improved the resistance of NBR to bubble formation under high-pressure hydrogen exposure compared to CNC-filled nanocomposites, demonstrating their superior suitability for such demanding applications. However, LCA revealed that both CNF and CNC nanocomposites currently entail relatively high environmental impacts, with Global Warming Potential (GWP) reaching up to 2.5 kg CO_2 eq. This underscores the importance of optimizing production processes to reduce their environmental footprint while maintaining performance benefits. Future work should focus on refining production methods to balance performance enhancements with reduced environmental impacts, paving the way for greener and more efficient hydrogen storage systems.

Author Contributions: S.Y. (Sheng Ye): Conceptualization, investigation, validation, writing, reviewing, and editing. S.Y. (Sohail Yasin): Conceptualization, investigation, validation, writing, reviewing, and Editing. H.Z.: Writing, reviewing, and editing. Y.S.: Validation, writing, reviewing, and editing. C.G.: Writing, reviewing, and editing. J.S.: Validation, writing, reviewing, and editing. All authors have read and agreed to the published version of the manuscript.

Funding: This work was supported by the National Natural Science Foundation of China (Grant No. 52475170).

Data Availability Statement: The original contributions presented in this study are included in the article. Further inquiries can be directed to the corresponding authors.

Conflicts of Interest: The authors declare no conflict of interest.

References

1. Yasin, S.; Shi, J.; Yihu, S.; Qi, C.; Yang, M.; Peng, W.; Zheng, C.; Li, Y.; Gu, C. Impacts of Deep Eutectic Solvent on Silica/Nitrile Rubber Nanocomposites for High-Pressure Hydrogen Storage Applications. *Compos. Commun.* **2024**, *46*, 101820. [CrossRef]
2. Zhou, C.; Liu, X.; Zheng, Y.; Hua, Z. A Comprehensive Review of Hydrogen-Induced Swelling in Rubber Composites. *Compos. Part B Eng.* **2024**, *275*, 111342. [CrossRef]
3. Castagnet, S.; Ono, H.; Benoit, G.; Fujiwara, H.; Nishimura, S. Swelling Measurement during Sorption and Decompression in a NBR Exposed to High-Pressure Hydrogen. *Int. J. Hydrogen Energy* **2017**, *42*, 19359–19366. [CrossRef]
4. Yasin, S.; Shi, J.; Ye, S.; Yihu, S.; Ullah, A.; Li, G.; Peng, W.; Gu, C. Sustainable Rubber Nanocomposites for Hydrogen Sealings: Impact of Carbon Nano-Onions and Bio-Based Plasticizer. *Polym. Degrad. Stab.* **2024**, *230*, 111051. [CrossRef]
5. Yasin, S.; Hafeez, M.; Hussain, M.; Mahmood, A.; Yihu, S.; Qiang, Z.; Gheewala, S.H.; Li, X.; Li, Y.; Shi, J.; et al. Cellulose Nanocrystal Filled Synthetic Rubber: Sustainable Production, Environmental Assessment and End-of-Life Biodegradation by Polyphagous Pests. *Sustain. Mater. Technol.* **2024**, *40*, e00947. [CrossRef]

6. Mohammad Taib, M.N.A.; Muhd Julkapli, N.; Yehye, W.A.; Abdul Hamid, S.B.O.A. Microstructures of Nanocellulose and Reinforcement in Nitrile Butadiene Rubber (NBR) Composites. *Solid State Phenom.* **2017**, *264*, 124–127. [CrossRef]
7. Dominic, M.; Joseph, R.; Begum, P.M.S.; Kumar, A.S.; Jeemol, P.A.; Jose, T.; Padmanabhan, D.; Formela, K.; Siengchin, S.; Parameswaranpillai, J.; et al. Cellulosic Bionanocomposites Based on Acrylonitrile Butadiene Rubber and Cuscuta Reflexa: Adjusting Structure-Properties Balance for Higher Performance. *Cellulose* **2021**, *28*, 7053–7073. [CrossRef]
8. Flory, P.J.; Rehner, J., Jr. Statistical Mechanics of Cross-linked Polymer Networks I. Rubberlike Elasticity. *J. Chem. Phys.* **1943**, *11*, 512–520. [CrossRef]
9. Flory, P.J.; Rehner, J. Statistical Mechanics of Cross-Linked Polymer Networks II. Swelling. *J. Chem. Phys.* **1943**, *11*, 521–526. [CrossRef]
10. Din, I.U.; Ahmed, A.; Tarek, F.; Cantwell, W.; Khan, K.A. Ultra-Thin Composites Membrane for Deployable Structures: XCT Driven Characterization and FE Modeling of Folding Structure. *Compos. Sci. Technol.* **2024**, *245*, 110341. [CrossRef]
11. Yasin, S.; Perwuelz, A.; Behary, N. A Case Study of Life Cycle Inventory of Cotton Curtain. In Proceedings of the 14th World Textile Conference Autex, Bursa, Turkey, 26–28 May 2014.
12. Bureau Veritas EIME, v6. Bureau Veritas. 2024. Available online: https://Codde.Fr/En/Our-Software/Eime-Presentation (accessed on 15 December 2024).
13. Yasin, S. Eco-Design for End-of-Life Phase of Flame Retardant Textiles. Ph.D. Thesis, Université Lille 1—Sciences et Technologies, Villeneuve-d'Ascq, France, 2017.
14. Yamabe, J.; Koga, A.; Nishimura, S. Failure Behavior of Rubber O-Ring under Cyclic Exposure to High-Pressure Hydrogen Gas. *Eng. Fail. Anal.* **2013**, *35*, 193–205. [CrossRef]
15. Fujiwara, H.; Yamabe, J.; Nishimura, S. Evaluation of the Change in Chemical Structure of Acrylonitrile Butadiene Rubber after High-Pressure Hydrogen Exposure. *Int. J. Hydrogen Energy* **2012**, *37*, 8729–8733. [CrossRef]
16. Yamabe, J.; Nishimura, S. Influence of Fillers on Hydrogen Penetration Properties and Blister Fracture of Rubber Composites for O-Ring Exposed to High-Pressure Hydrogen Gas. *Int. J. Hydrogen Energy* **2009**, *34*, 1977–1989. [CrossRef]
17. Roy, K.; Pongwisuthiruchte, A.; Debnath, S.C.; Potiyaraj, P. Application of Cellulose as Green Filler for the Development of Sustainable Rubber Technology. *Curr. Res. Green Sustain. Chem.* **2021**, *4*, 100140. [CrossRef]
18. Faye, A.; Rodríguez-Martínez, J.A.; Volokh, K.Y. Spherical Void Expansion in Rubber-like Materials: The Stabilizing Effects of Viscosity and Inertia. *Int. J. Non-Linear Mech.* **2017**, *92*, 118–126. [CrossRef]
19. Mo, L.; Xiao, X.; Chen, Y.; Fang, M.; Xiao, S.; Yong, H.; Li, C.; Chen, C. A Rapid Decompression Failure Mechanism Model Coupling Diffusion-Deformation of O-Ring Sealing Rubber Exposed to High-Pressure Carbon Dioxide. *Eng. Fail. Anal.* **2025**, *170*, 109271. [CrossRef]
20. Visakh, P.M.; Thomas, S.; Oksman, K.; Mathew, A.P. Crosslinked Natural Rubber Nanocomposites Reinforced with Cellulose Whiskers Isolated from Bamboo Waste: Processing and Mechanical/Thermal Properties. *Compos. Part A Appl. Sci. Manuf.* **2012**, *43*, 735–741. [CrossRef]
21. Chen, Y.; Zhang, Y.; Xu, C.; Cao, X. Cellulose Nanocrystals Reinforced Foamed Nitrile Rubber Nanocomposites. *Carbohydr. Polym.* **2015**, *130*, 149–154. [CrossRef] [PubMed]
22. Taib, M.N.A.M.; Yehye, W.A.; Julkapli, N.M. Influence of Crosslinking Density on Antioxidant Nanocellulose in Bio-Degradation and Mechanical Properties of Nitrile Rubber Composites. *Fibers Polym.* **2019**, *20*, 165–176. [CrossRef]
23. Bhattacharjee, S.; Bhowmick, A.K.; Avasthi, B.N. High-Pressure Hydrogenation of Nitrile Rubber: Thermodynamics and Kinetics. *Ind. Eng. Chem. Res.* **1991**, *30*, 1086–1092. [CrossRef]
24. Fujiwara, H.; Ono, H.; Nishimura, S. Degradation Behavior of Acrylonitrile Butadiene Rubber after Cyclic High-Pressure Hydrogen Exposure. *Int. J. Hydrogen Energy* **2015**, *40*, 2025–2034. [CrossRef]
25. Gopalan Nair, K.; Dufresne, A. Crab Shell Chitin Whisker Reinforced Natural Rubber Nanocomposites. 1. Processing and Swelling Behavior. *Biomacromolecules* **2003**, *4*, 657–665. [CrossRef] [PubMed]
26. Yasin, S.; Hussain, M.; Zheng, Q.; Song, Y. Effects of Ionic Liquid on Cellulosic Nanofiller Filled Natural Rubber Bionanocomposites. *J. Colloid Interface Sci.* **2021**, *591*, 409–417. [CrossRef] [PubMed]
27. Poh, G.K.X.; Chew, I.M.L.; Tan, J. Life Cycle Optimization for Synthetic Rubber Glove Manufacturing. *Chem. Eng. Technol.* **2019**, *42*, 1771–1779. [CrossRef]
28. Yasin, S.; Hussain, M.; Zheng, Q.; Song, Y. Thermo-Soil Weathering and Life Cycle Assessment of Carbon Black, Silica and Cellulose Nanocrystal Filled Rubber Nanocomposites. *Sci. Total Environ.* **2022**, *835*, 155521. [CrossRef]
29. Pyay, S.; Thanungkano, W.; Mungkalasiri, J.; Musikavong, C. A Life Cycle Assessment of Intermediate Rubber Products in Thailand from the Product Environmental Footprint Perspective. *J. Clean. Prod.* **2019**, *237*, 117632. [CrossRef]

30. ICCA. *Avoiding Greenhouse Gas Emissions: The Essential Role of Chemicals: Life Cycle Assessment of Circular Systems*; International Council of Chemical Associations (ICCA): Brussels, Belgium, 2021.
31. Foroughi, F.; Rezvani Ghomi, E.; Morshedi Dehaghi, F.; Borayek, R.; Ramakrishna, S. A Review on the Life Cycle Assessment of Cellulose: From Properties to the Potential of Making It a Low Carbon Material. *Materials* **2021**, *14*, 714. [CrossRef]

Disclaimer/Publisher's Note: The statements, opinions and data contained in all publications are solely those of the individual author(s) and contributor(s) and not of MDPI and/or the editor(s). MDPI and/or the editor(s) disclaim responsibility for any injury to people or property resulting from any ideas, methods, instructions or products referred to in the content.